New Cathode Material for Air-Plasma Cutting (Report III)†

— Effect of Thermal and Electric Properties of Ru-Y_2O_3 on Electrode Consumption —

Fukuhisa MATSUDA* Masao USHIO* and Kazuomi KUSUMOTO**

Abstract

This paper describes physical properties for sintered Ru-Y_2O_3 system, Zr and Hf; thermal properties (thermal diffusivity, specific heat and thermal conductivity) and electrical resistivity. And explains the relationship between its physical properties and electrode consumption.

80Ru-20Y_2O_3 electrode which has superior erosion resistance showed high thermal and electric conductivity at room temperature comparing with those of Zr and Hf electrodes.

KEY WORDS: (Air-Plasma Cutting) (Ruthenium, Yttrium-Oxide) (Laser Flash Method) (Thermal Diffusivity) (Specific Heat) (Thermal Conductivity) (Electrical Resistivity)

1. Introduction

The consumption rate of cathode material used in air plasma cutting may be related to its physical properties and as well as to the cooling gain of the cathode.

On the physical properties of cathode materials, the most relevant ones are thermal and electrical conductivities of bulk itself and the surface properties related with the electron emission and the interraction with oxygen.

This paper describes the effect of the thermal properties and the electrical resistivity of a sintered Ru-Y_2O_3 system on the electrode consumption. And it was referred to Zr and Hf made by sintering and melting processes.

2. Materials and Measurement Method

2.1 Measurement of thermal properties

Materials used in this study were shown in **Table. 1**. Ru-Y_2O_3 system were sintered at 2273 K for 1.8 ks in hydrogen atmosphere. Two kinds of Zr were prepared by sintering at 1373 K for 3.6 ks in vacuum and by melting process respectively. And also two kinds of Hf were prepared by sintering at 1773 K for 1.8 ks in vacuum and by melting process. The thermal properties were measured by laser flash method[1)].

Specimen size is 8.8 mm in a diameter, 1.7 mm in a thickness and the both sides of the specimen surface were mechanically polished. After that, C-A thermocouple (50 μm in a diameter) were attached on the center of the reverse side of the specimen surface with a silver paste.

Table 1 Processing conditions and average density ratio of samples.

Material	Processing conditions	Av.density ratio(%)
Zr	Melting material	98.8
Zr	Sintering 1373K×3.6ks in Vac.	93.5 ~ 93.7
Hf	Melting material	96.8
Hf	Sintering 1773K×1.8ks in Vac.	82.1 ~ 83.3
Ru	Sintering 2373K×1.8ks in H_2	95.6 ~ 96.0
95Ru- 5Y_2O_3		92.8 ~ 93.3
80Ru-20Y_2O_3		98.0 ~ 98.3
60Ru-40Y_2O_3		97.3 ~ 98.7

In the measurement of thermal diffusivity, the polished surface was exposed to the laser beam flashed as shown in **Fig. 1 (a)**. But in the measurement of specific heat, a thin sheet of grassy carbon was attached on the specimen surface with a silicon grease so that the absorptivities of variable specimens may be same as shown in **Fig. 1 (b)**.

Figure 2 (a) shows the schematic diagram of the laser flash method. When the laser beam is flashed in the specimen surface, the temperature rise on the reverse side of the specimen surface is described as shown in **Fig. 2 (b)**. From this curve, the thermal diffusivity α[cm²/sec] is calculated as follows.

$$\alpha = \frac{1.37L^2}{\pi^2 t_{1/2}} \qquad (1)$$

Here, L: Thickness of specimen [cm]

† Recieved on November 30, 1990

* Professor

** Graduate Student, Osaka University

Transactions of JWRI is published by Welding Research Institute of Osaka University, Ibaraki, Osaka 567, Japan

$t_{1/2}$: Time needed to reach the half value of maximum temperature at the reverse side of specimen [sec].

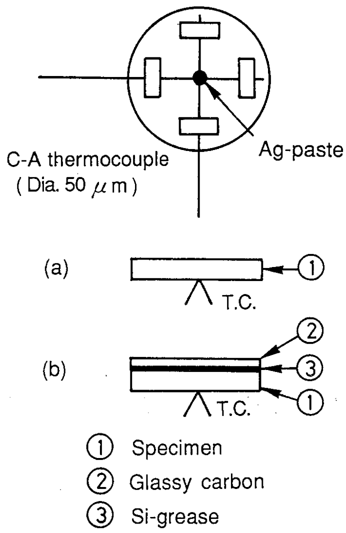

Fig. 1 Illustration of specimens for measurement of thermal properties by laser flash method.
(a) for thermal diffusivity
(b) for specific heat.

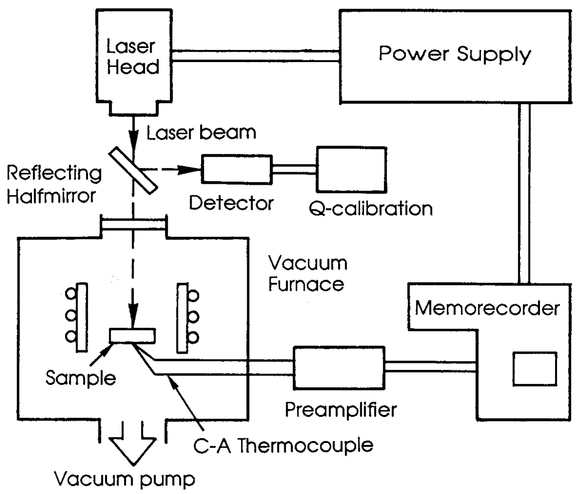

Fig. 2(a) Schematic diagram of thermal properties measurement by laser flash method.

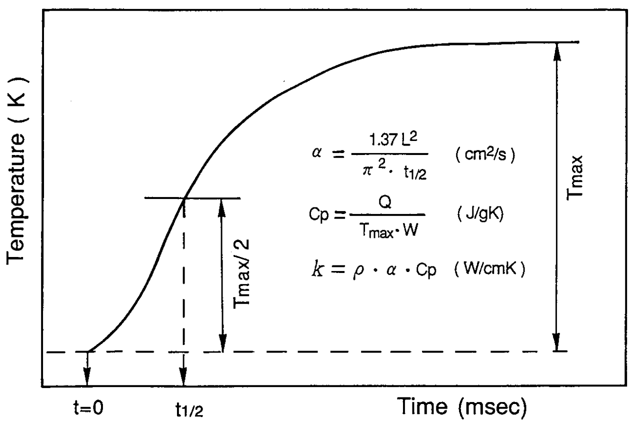

Fig. 2(b) Temperature change at reverse side surface of specimen.

And the specific heat *Cp* [*J/gK*] is calculated from the next equation (2).

$$Cp = \frac{1}{W}\left(\frac{Q}{T_{max}} - Wc \cdot Cpc - Wg \cdot Cpg\right) \qquad (2)$$

Here, T_{max}: Temperature at the reverse dise of specimen [K]

Q: Input of laser power [J]

W: Weight of specimen [g]

Wc: Weight of grassy carbon [g]

Wg: Weight of silicon grease [g]

Cpc: Specific heat of glassy carbon [J/gK]

Cpg: Specific heat of silicon grease [J/gK].

Then, the thermal conductivity k [W/cmK] is calculated from equations (1) and (2).

$$k = \alpha \cdot \rho \cdot Cp \qquad (3)$$

Here, ρ is the density of specimen (g/cm^3).
All measurement were carried out at room temperature.

2.2 Measurement of electrical resistivity

Specimen were made by the same sintering condition as one for the measurement of thermal conductivity but the size was $15 \times 10 \times 2^t$ as shown in **Fig. 3**.

The electrical resistivity was measured by the four terminal method at room temperature.

3. Experimental Results and Discussions

3.1 Thermal diffusivity and specific heat

The thermal diffusivity of Ru-Y_2O_3 system is shown in **Fig. 4**. The present data are an average value of three measurements for each specimen. The thermal diffusivity was decreased with increasing Y_2O_3 content

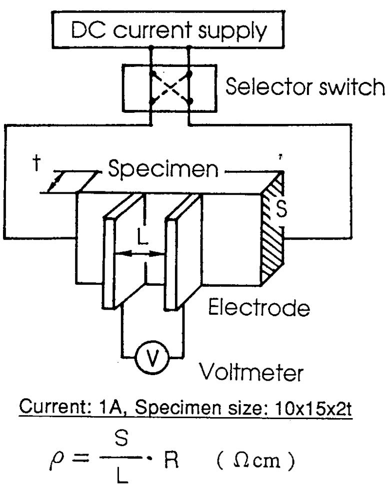

Fig. 3 Schematic diagram of electrical resistivity measurement.

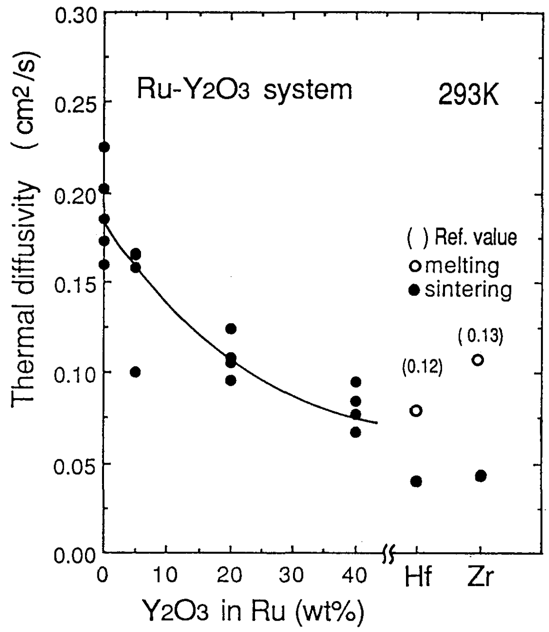

Fig. 4 Thermal diffusivity of Ru-Y_2O_3 system at room temperature.

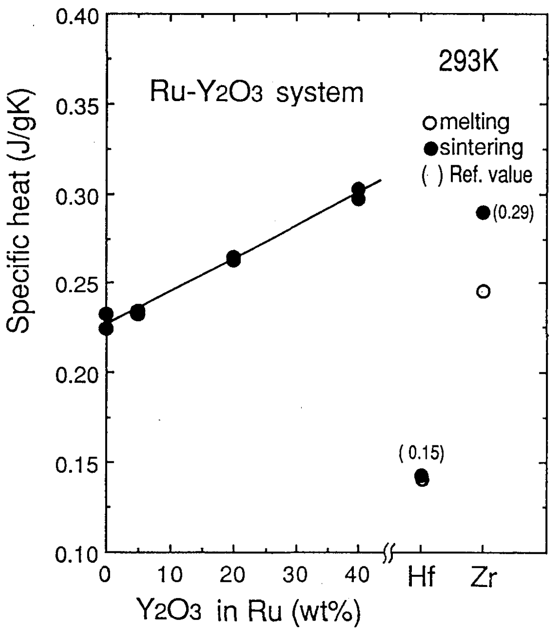

Fig. 5 Specific heat of Ru-Y_2O_3 system at room temperature.

in Ru. 100Ru one showed the value of about 50% of the reference value (0.403 cm^2/sec) of polycrystalline[2]. In cases of Zr and Hf, the sintered products showed low diffusivities comparing with the melted ones. It may be considered that pores in the sintered body act as barriers of thermal diffusion.

In **Fig. 5**, the specific heat at room temperature is plotted versus Y_2O_3 content in Ru. The specific heat of Ru-Y_2O_3 system is slightly increased with increasing Y_2O_3 content. In the case of Hf, the specific heat of the sintered product was a same value as the melted one. In the case of Zr, the specific heat of the sintered product was higher than that of the melted one.

3.2 Thermal conductivity

Figure 6 shows the thermal conductivity of the sintered Ru-Y_2O_3 system calculated from the equation (3). The thermal conductivity was decreased with increasing Y_2O_3 content in Ru. In a previous study[3], it could be estimated that the thermal conductivity of Ru-Y_2O_3 electrode of above around 40 wt% in Y_2O_3 content decreases rapidly from the results of the electrode consumption test. However, the conductivity was moderately decreased with increasing Y_2O_3 content in reality. In the cases of Zr and Hf, the thermal conductivity of sintered products were lower than those of melted products.

It can be considered that the thermal conductivity is directly influenced by the thermal diffusivity which is closely related with the pore in the sintered bulk. **Figure 7** and **8** show the fracture surface of sintered Zr, Hf and Ru-Y_2O_3 system observed by using SEM. The following observations can be explained:

(1) The sintered Zr indicates the typical transgranular fracture with the round pore, probably due to the high densification.

On the other hand, the sintered Hf indicates the typical intergranular fracture with a large number of the elongated pore. This is because of the imperfect densification.

(2) In the case of 100Ru, the intergranular cracking as an ice candy with the large grain growth could be seen. This is relatively higher temperature of sintering than those of Zr and Hf.

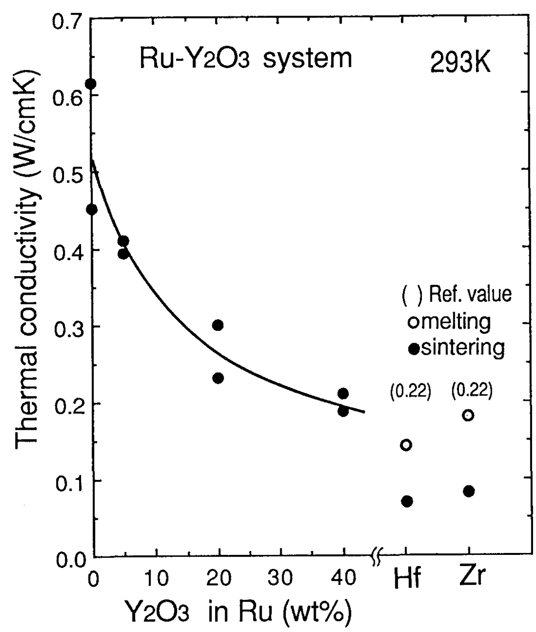

Fig. 6 Thermal conductivity of Ru-Y_2O_3 system at room temperature.

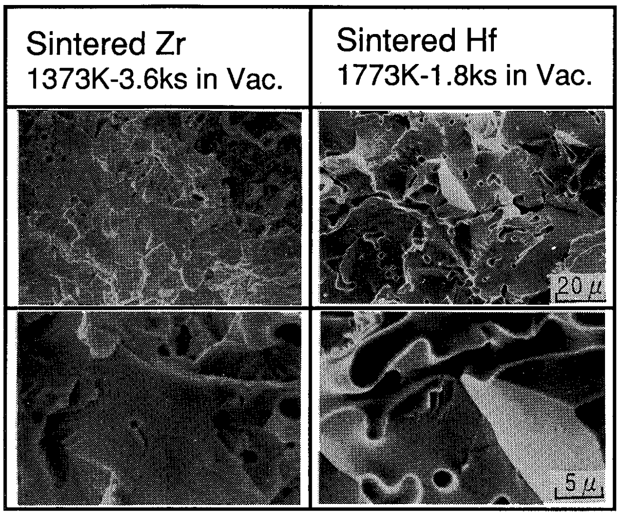

Fig. 7 Fracture surface of sintered products [Zr and Hf].

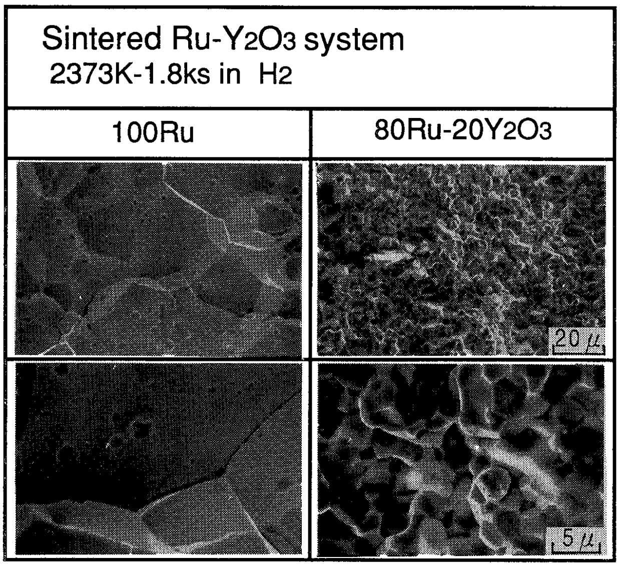

Fig. 8 Fracture surface of sintered Ru-Y_2O_3 system.

On the other hand, the sintered Ru including Y_2O_3 shows the densificated microstructure comparing with 100Ru. It can be considered that Y_2O_3 prevents from the grain growth of Ru.

3.3 Electrical resistivity

Figure 9 shows the relationship between the electrical resistivity at room temperature and Y_2O_3 content in Ru. The electrical resistivity increases slightly with increasing Y_2O_3 content in the range of small amounts of Y_2O_3. This is due to the characterizing mainly metallic conduction. Above around 50 wt% in Y_2O_3 content, the resistivity increases rapidly. It is considered that the conduction mechanism changes from the metallic conduction to the non-metallic one. Then, the electical resistivity of Ru including 60 wt% in Y_2O_3 was measured by using the three terminal method which is

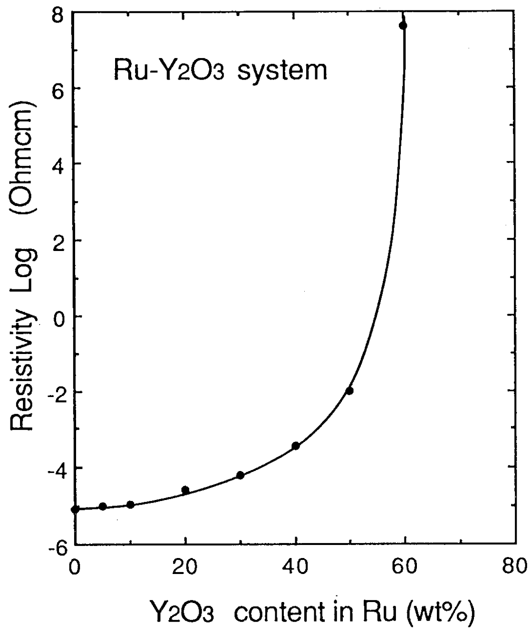

Fig. 9 Relationship between electrical resistivity and Y_2O_3 content in Ru.

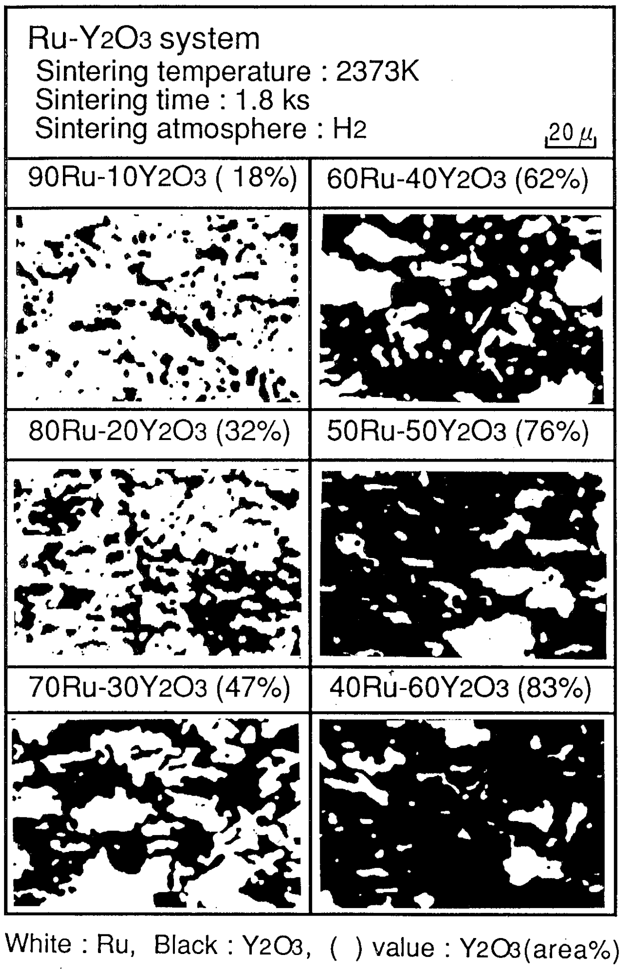

Fig. 10 Microstructure of Ru-Y_2O_3 system obtained by digital treatment.

widely used for the measurement of insulators.

It may be considered that the characteristics of resistivity mainly depends on the distribution of Ru and Y_2O_3 components. **Figure 10** shows the microstructure obtained with the digital treatment which showed the white part corresponding to Ru component and the black part corresponding to Y_2O_3 component. And the value of round brackets shows the surface area percent for the black part (Y_2O_3). In this figure, until around 20 wt% in Y_2O_3 content, Ru component links with a continuous electric circuit. And the metallic part decreases with increasing Y_2O_3 content. Above around 50 wt% in Y_2O_3, Ru component is apparently isolated each other in Y_2O_3 such as the interrupted electric circuit. In aspect of the three dimension, it may be considered that Ru component slightly plays a role of electric conduction.

3.4 Relationship between electrode consumption and its physical properties.

Figure 11 shows the relationship between the electrode consumption (electrode weight loss) and its physical properties such as the thermal conductivity and the electrical resistivity for Ru-Y_2O_3 electrode. The consumption data was obtained under 25 A in arc current and 0.3 ks in operating time by using air in operating gas[3]. It can be pointed out as follows: (1) Below around 5 wt% in Y_2O_3 content, the consumption was severely high. (2) The electrode consumption showed a minimum value in the range from 5 to 30 wt% in Y_2O_3 content. (3) Above 30 wt% in Y_2O_3 content, the consumption was severely progressed.

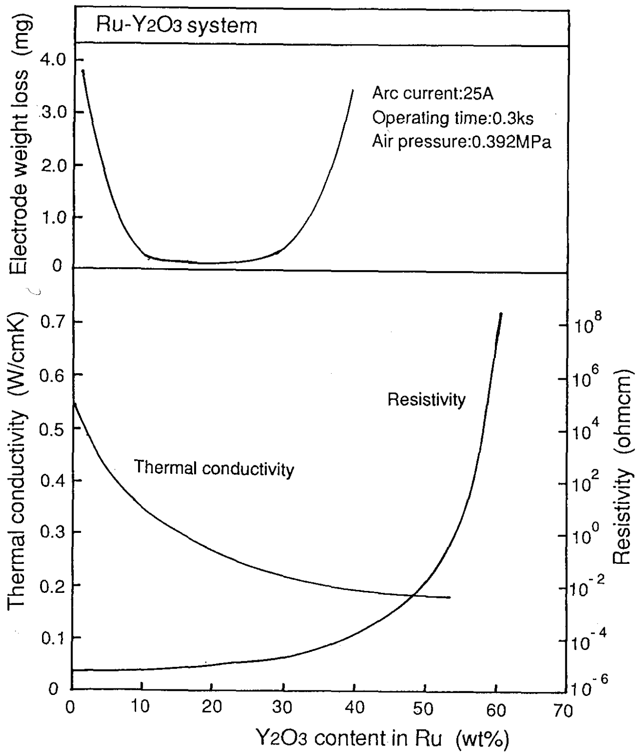

Fig. 11 Relationship between thermal and electrical properties and electrode weight loss for Ru-Y_2O_3 system.

The consumption characteristic in the case of above 30 wt% in Y_2O_3 content could be explained as the insufficient thermal and electric conductions due to the increased volume fraction of Y_2O_3.

But the consumption characteristic in the case of below 5 wt% in Y_2O_3 content can not be explained by the thermal and electric properties of the bulk. It may be attributable to Y_2O_3 action related with the thermionic emission and the oxidization on the cathode surface.

From the previous study, 80Ru-20Y_2O_3 was one of the acceptable electrode in Ru-Y_2O_3 system. Then comparing the thermal conductivity and electrical resistivity of 80Ru-20Y_2O_3 electrode with those of Zr and Hf, the thermal conductivity of 80Ru-20Y_2O_3 (0.266 W/cmK) was higher than those of Zr (0.226 W/cmK) and Hf (0.229 W/cmK)[4], and the electrical resistivity of 80Ru-20Y_2O_3 (23 $\mu\Omega$ cm) was lower than those of Zr (44 $\mu\Omega$ cm) and Hf (32.2 $\mu\Omega$ cm)[4]. Therefore, it is clear that 80Ru-20Y_2O_3 electrode has high thermal and electric conductions comparing with Zr and Hf.

4. Conclusions

The main conclusions drawn from this study are as follows:

(1) The thermal diffusivity and conductivity of sintered Hf and Zr were lower than those of melted Hf and Zr.

(2) 80Ru-20Y_2O_3 showed relatively high thermal and electric conductions compared with Zr and Hf which have been widely used in the electrode materials for air plasma cutting torch.

(3) The consumption above around 30 wt% in Y_2O_3 content in Ru was considered to be strongly related with the severe increase of the electrical resistivity.

Acknowledgements

The authors would like to express their appreciation to TOHO KINZOKU CO., LTD. for production of the specimen. This study was partially supported by Grant-in-Aid for Scientific Research of the Ministry of Education in Japan (No. 02952179).

References

1) W.J. Parker, R.J. Jenkins, C.P. Butler and G.L. Abott: J. Appl. Phys. 32 (1961) 1679.

2) Thermal diffusivity, Thermophysical Properties of Matter, The TPRC Data Series Vol 10, (1973), IFI/PLENUM.
3) F. MATSUDA, M. USHIO and K. KUSUMOTO, Trans. of JWRI. 18 (1989), p 127.
4) C.J. Smithells and E.A. Brandes, Metals Reference Book, 5th ed. (1976), Butterworths.